

Published in final edited form as:

Mol Pharm. 2013 June 3; 10(6): 2331–2339. doi:10.1021/mp3007083.

Effect of formulation pH on transport of naltrexone species and pore closure in microneedle-enhanced transdermal drug delivery

Priyanka Ghosh^{a,b}, Nicole K. Brogden^{a,c}, and Audra L. Stinchcomb^{a,b,d,*}

^aDepartment of Pharmaceutical Sciences, College of Pharmacy, University of Kentucky, Lexington, KY 40536-0082, USA

^bDepartment of Pharmaceutical Sciences, School of Pharmacy, University of Maryland, Baltimore, MD 21201, USA

^dAllTranz, Inc., Lexington, KY 40505, USA

Abstract

Microneedle-enhanced transdermal drug delivery greatly improves the subset of pharmacologically active molecules that can be transported across the skin. Formulation pH plays an important role in all drug delivery systems; however, for transdermal delivery it becomes specifically significant since a wide range of pH values can be exploited for patch formulation as long as it does not lead to skin irritation or sensitization issues. Wound healing literature has shown significant pH effects on barrier recovery. Stability and solubility of the drug, and thus transport across skin are all affected by formulation pH. The current study examined the role of ionization state of the drug naltrexone on transdermal flux and permeability across microneedle treated skin, as compared to intact skin. Impedance spectroscopy was done in pigs *in vivo* to assess the role of formulation pH on the rate of micropore closure under the influence of three different pH conditions. The data indicated that while there was significant advantage of using a lower pH formulation in terms of total transport across microneedle treated skin, the pH however did not have any significant effect on the rate of micropore closure beyond the first 24 hours.

Keywords

Microneedle; micropore closure; permeability; transdermal; impedance spectroscopy

Introduction

Skin is the largest and the most accessible organ of the body. The extensive vasculature in the dermal region of the skin ensures rapid uptake of any compound that is transported across the skin into the systemic circulation, thus making the skin a very attractive drug delivery target^{1,2}. However, in order to protect an individual's internal environment from

*Corresponding author: Audra L. Stinchcomb, PhD, Professor, Department of Pharmaceutical Sciences, University of Maryland School of Pharmacy, 20 N. Pine St., Baltimore, MD 21201, USA, Phone: (410) 706 – 2646, Fax: (410) 706 – 0886, astinchc@rx.umaryland.edu.

^cDepartment of Pharmaceutical Sciences and Experimental Therapeutics, College of Pharmacy, University of Iowa, Iowa City, IA-52242, USA (Current address)

Conflict of Interest:

Audra Stinchcomb is Chief Scientific Officer and Founder of AllTranz Inc, a transdermal specialty pharmaceutical company developing microneedle formulations.

infiltration of xenobiotics as well as excessive water loss, the stratum corneum (SC), the topmost layer of the skin is specifically designed to protect the human body³. A very small subset of pharmacologically active molecules can successfully cross the SC (passive delivery) in therapeutically relevant concentrations^{2,4}. Research in the field of passive transdermal delivery has focused primarily on small molecular weight (<500Da) unionized compounds with a octanol/water partition coefficient ($\log P$)~2 to help in transport and partitioning across the SC, the most important barrier to passive transport^{1,5}. Active transdermal drug delivery systems on the other hand employ some kind of physical enhancement technique to permeablize the SC or reduce the barrier effect of the SC. Research and development in the field of active drug delivery systems over the past two decades have greatly enhanced the number of molecules that can be delivered transdermally. It has also opened up a whole new area of research since active transdermal systems focus on transport across the lower epidermal and dermal layers, which are more hydrophilic than the SC and could benefit from water-soluble drug candidates^{2,6,7}.

The current study focuses on microneedle (MN) enhanced transdermal drug delivery as a model of active drug delivery systems. Other active drug delivery systems may include iontophoresis, ultrasound, microdermabrasion, or electroporation. MN's are small micron-scale needles that are used to permeablize the skin by creating micropores or microchannels across the SC⁸. Once the SC barrier is removed, drug can directly pass into the interstitial fluid and the lower layers of the skin. MN can vary in length anywhere from 200 μm to a few millimeters. There are four different methods of MN application, "poke/press and patch" where solid MN are used to permeablize the skin followed by application of a drug patch, coated MN where drug is coated onto the surface of the MN and used as the drug delivery medium, dissolving MN where drug is loaded into the polymer used for MN synthesis, and hollow MN where drug is pushed through micron-scale needles with the help of an infusion pump. Several researchers have looked at the effects of needle length, needle shape, material, etc. on the mechanical/structural integrity of MN^{9,10}. Additional studies have focused on transport and drug delivery across MN treated skin both *in vitro* as well as *in vivo*. It has been shown that a large number of molecules can be successfully delivered using a MN system. Some examples include naltrexone, calcein, insulin, parathyroid hormone, etc.¹¹⁻¹³

Formulation and pore closure kinetics for MN enhanced drug delivery had not been investigated in great depth until recently. The effect of charge/ionization state was investigated by Banks et al. to show that an ionized form of the drug exhibited a higher flux using naltrexone (NTX) and naltrexol. For intact skin, it is known that unionized molecules generally exhibit faster transport, but in MN treated skin the primary permeation route is completely different and the faster transport of ionized molecules was an important finding. In the Banks study it was concluded that the faster transport of ionized molecules could be attributed to enhanced solubility¹¹. Another aspect of MN formulation that has been investigated is the effect of formulation viscosity. Milewski et al. showed that a lower viscosity formulation translated into faster flux compared to a higher viscosity propylene glycol (PG) rich formulation utilizing the same concentration of drug in the donor. The results in that study could be explained by assuming a Stokes-Einstein equation for diffusivity of drug through the MN pores instead of the free volume theory that is used for intact skin¹⁴. The third aspect of donor formulation investigated was the effect of saturation on transport across MN pores. For intact skin, delivery from a saturated solution translates into the maximum driving force and hence the fastest flux. However, in MN enhanced delivery it has been shown that the highest flux is achieved using a sub-saturated solution due to pore clogging and viscosity effects¹⁴⁻¹⁶.

MN enhanced delivery maximizes drug transport by creating micropores (or microchannels) across the skin. However, these micropores begin to close under the influence of normal physiological functions. Thus the efficacy of sustained-release MN enhanced delivery is greatly limited by the lifetime of the micropores. Recent literature reports have shown the effect of MN geometry, occlusion, and skin type on the rate of pore closure. Several direct and surrogate markers have been used by different groups for closure rate comparison, such as transepidermal water loss (TEWL), impedance spectroscopy, dye imaging, and pharmacokinetics^{11, 17–20}. By and large, a pore closure timeframe of 48–72 hours under occlusion and around 10–15 minutes without occlusion has been observed. Several factors may contribute to the closure of micropores. The formation of the SC depends on the availability of SC lipids, their processing and release from lamellar bodies²¹. Deeper tissue wound healing is a multi-step process which involves inflammation, proliferation and remodeling²². The role of pH in healing of superficial wounds due to tape stripping or acetone treatment has been previously studied using TEWL in rat skin. The results from those studies showed that healing of the skin is delayed at a higher pH of 7.4.²³ The results can be explained in terms of activity of β -glucocerebrosidase across the pH range of the study from 5.5–7.4. β -glucocerebrosidase is an important enzyme in the ceramide synthesis pathway²⁴, and exhibits an activity maximum around pH 5, with substantially decreased activity at pH 7.4²⁵. Since ceramides constitute 50% of the SC structure by weight, and a molar ratio of 1:1:1 of ceramides: cholesterol: fatty acids is an important factor for proper formation of the SC barrier, at a higher pH the rate of healing is significantly slower over a 6 hour timeframe^{26, 27}. The effect of surface pH in chronic wounds has also been studied^{28, 29}.

There are several factors that can contribute to transport and pore closure during MN enhanced delivery. The effect of formulation pH was examined in this study. The model compound of choice was NTX (molecular weight- 341.4, log P- 2.0, pKa- 7.5, 9.16)³⁰. It is a μ -opioid receptor antagonist used in alcohol and opioid addiction³¹. ReVia[®], the original daily oral formulation has bioavailability issues as well as gastrointestinal side effects³². Vivitrol[®], the extended release 28-day formulation has injection site reactions, and it is difficult to remove if emergency opioid treatment is required³³. Hence, NTX is a good model compound for a sustained release transdermal patch formulation. NTX does not reach a therapeutically relevant plasma concentration via passive transdermal delivery, so MN enhanced drug delivery was used for development of an active transdermal patch. The first human study with NTX and MN showed that while utilizing MN, drug could be delivered in the lower therapeutic plasma level range for 48–72h, no detectable level of the drug was obtained in plasma for the control non-MN treated subjects³⁴. Subsequent efforts were directed towards improving the NTX formulation for better transport, as well as enhancement of pore lifetime by using diclofenac sodium towards the development of a 7 day transdermal system, the ideal transdermal drug delivery goal^{14, 16, 20, 35–39}. In this study the effect of formulation pH will be evaluated for transport and in depth analysis of permeability via the microchannel pathway and intact skin pathway. A mechanistic understanding of the relation between ionization state and transdermal flux will help in development of active transdermal systems for a host of different molecules that can potentially benefit from a multiday sustained release dosage form. Since the factors contributing to micropore closure are not very well understood yet, studying the effect of formulation pH on micropore closure kinetics will help determine if this can be used as a possible mechanism for pore lifetime enhancement for development of 7-day drug delivery systems.

Experimental section

2.1 Chemicals

Naltrexone base was purchased from Mallinckrodt (St. Louis, MO). Citric acid monohydrate was purchased from Fisher chemicals (Fairlawn, NJ). Water was purified using a NANO pure Diamond™, Barnstead water filtration system. 1-Octanesulfonate, sodium salt was obtained from Regis Technologies, Inc. (Morton Grove, IL). Trifluoroacetic acid (TFA), triethylamine (TEA) and acetonitrile (ACN) were obtained from EMD chemicals (Gibbstown, NJ). Sodium hydroxide was obtained from Sigma (Saint Louis, MO). Natrosol® (hydroxyethylcellulose) was obtained from Ashland (Wilmington, DE). Seventy percent ethanol was obtained from Ricca chemicals (Arlington, TX)

2.2 Donor solution preparation

All donor solutions for *in vitro* permeation studies were prepared in citrate buffer (0.3M). Citric acid monohydrate was mixed with nanopure water to obtain a base solution. The pH was then adjusted with sodium hydroxide to obtain solutions at 6 different pH values (pH 5.76, pH 6.30, pH 6.43, pH 6.72, pH 7.56, pH 8.26). NTX base was added to 3ml of each solution in excess, vortexed, sonicated for 10 minutes, and were left in a shaker water bath at 32°C overnight. The pH adjusted saturated drug solutions were used as donor solutions for all studies.

All donor gels for *in vivo* pig studies were prepared in citrate buffer (0.1M). Citric acid monohydrate was used to prepare a base solution. The pH was adjusted to pH 5.5, pH 6.5 and pH 7.4 using NaOH (3M). The solutions were left overnight and the pH was also measured on the next day to make sure changes did not occur. Three percent hydroxyethylcellulose (HEC) was added to each solution as a gelling agent. The gels were stored at 32°C for the entire length on the study.

2.3 pH measurements

The pH of all *in vitro* donor solutions were measured using a VWR® sympHony® (SB70P) pH meter and VWR® sympHony® Glass Combination pH Electrode. All solutions were measured following pH adjustment, after overnight incubation with drug, and immediately before dosing.

2.4 Solubility determination

The apparent solubility of NTX base in solutions with different pH values was determined immediately prior to dosing. Five hundred µl of each donor solution was filtered using a 0.2µm, 500µl centrifugal filter. Ten µl of the filtered solutions was used to spike 10ml of ACN. Concentration of drug was analyzed using a HPLC (method reported in quantitative analysis section) after appropriate dilutions. All solubility determination experiments were carried out in triplicate.

2.5 Viscosity measurements

Viscosity was measured using a Brookfield DV-III LV programmable cone/plate rheometer and a CPE-40 spindle. Each filtered donor solution viscosity was measured at three different torque values within the range of 10–100% torque. The temperature was maintained at 32°C using a circulating water bath throughout the study.

2.6 *In vitro* diffusion studies

Full thickness Yucatan miniature pig skin was used for all *in vitro* experiments. The skin was removed from euthanized animals under a University of Kentucky IACUC approved

protocol. The skin was obtained from the dorsal region of euthanized animals, dermatomed to a thickness of 1.4–1.8mm after removal of all subcutaneous fat and frozen (at -20°C) until use. Skin samples were thawed on the day of the study. For MN treatment, the skin was placed on a wafer of Sylguard[®] 184 silicone elastomer to mimic the underlying tissue. MNs for this study were obtained from Dr. Mark Prausnitz's laboratory at the Georgia Institute of Technology. A 5 MN in plane MN array was used for *in vitro* studies. Each MN was 750 μm long, 200 μm wide and 75 μm thick and the inter needle spacing was 1.35 μm . Each square piece of skin was pierced 20 times to create a total of 100 MN pores (Skin was rotated by 90° following 10 MN insertions so as to create non-overlapping pores). The skin was then placed in a horizontal flow through diffusion cell with an active diffusion area of 0.95 cm^2 . Untreated skin was placed directly onto the diffusion cells. Three to four cells were used per treatment group for all experiments. A PermeGear flow through (In-line, Riegelsville, PA) cell was used for *in vitro* diffusion studies. Water adjusted to pH 7.4 containing 20% ethanol was used as the receiver solution. The flow rate of the receiver solution was adjusted to 1.5ml/h to maintain sink conditions. The temperature of the cells was maintained at 32°C , the temperature of the outer surface of the skin. Transepidermal water loss (TEWL) measurements were obtained to make sure that untreated skin had values $<5\text{g}/\text{m}^2/\text{h}$ indicating no damage. Each cell was charged with 250 μl of saturated donor solution and receiver solution was collected in 6h increments for a total of 48h. Drug concentration was quantified using a HPLC assay for NTX. A cumulative amount vs. time plot was generated and flux was determined from the steady state portion of the curve using Fick's first law of diffusion.

$$J_{TOT} \text{ OR } J_{SS} = \frac{1}{A} \left(\frac{dM}{dt} \right) = P * S_{TOT}$$

J_{TOT} or J_{SS} is the steady state flux or total flux, A is the diffusional surface area (0.95 cm^2), M is the total mass transport across a membrane (skin in this case) and t is time. P is the apparent permeability coefficient and S_{TOT} is the saturation solubility of the donor. The driving force for diffusion is the concentration gradient across the barrier. However, in this case since the receiver solution is maintained at sink conditions throughout the experiment, the driving force is the solubility of the drug in the donor. Flux enhancement is the ratio of flux across MN treated skin to flux across non treated skin for the same formulation. At the end of the experiment, the skin was removed and dissected into small pieces. Skin concentration of drug was measured by extracting drug from the tissue into ACN overnight at 32°C and analyzing the solution by HPLC after appropriate dilutions.

2.7 Quantitative analysis

The drug concentration in the receiver solution was measured using a HPLC assay. The HPLC system consisted of Waters 2695 separation module, Waters 2489 dual wavelength absorbance detector and Waters Empower[™] software. A Perkin Elmer Spheri5 VL C18 column (5 μ , 220 \times 4.6mm), C18 guard column (15 \times 3.2mm) was used. The mobile phase consisted of 70:30(v/v) of ACN: 0.1% TFA containing 0.065% 1-octane sulfonic acid sodium salt, adjusted to pH 3.0 with TEA aqueous phase. The wavelength used for quantification was 280nm. The injection volume for all samples was 100 μl and the retention time for NTX was 2.1 ± 0.1 min. Samples were analyzed within a 100–10000 ng/ml linear range of standard curve (r^2 0.99)

2.8 *In vivo* studies with impedance spectroscopy

Impedance spectroscopy was used to look at pore closure kinetics in the Yucatan miniature pig. All animal experiments were approved by the University of Kentucky IACUC. The pig

skin was cleaned with soap and water a day before the treatment. On the day of the treatment, all sites were marked, 3 sites for MN treatment and 1 site for intact skin control for each formulation. The site for the reference electrode was in the center and equidistant from all measurement sites. The impedance setup consisted of an impedance meter (EIM-105 Prep-Check), 200 k Ω resistor in parallel (IET labs, Inc.), reference and measurement electrodes. A large electrode (70mm diameter) with conductive gel (Superior StarBurst® electrode with PermaGel) was used as the reference electrode. A Ag/AgCl gel electrode (S & W Healthcare Corp. Series 800, 50mm diameter total area, 10 mm active electrode diameter) was used as the measurement electrode. Baseline measurements were obtained in duplicate at all 12 sites⁴⁰. Active sites were cleaned with an ethanol swab, allowed to dry and treated twice with a 50 MN array (to give a total of 100MN insertions). The sites were measured again for post-MN treatment value; 200 μ l of gel was then applied to each site and covered with an occlusive patch⁴¹. The non-treated control sites were occluded after application of gel as well. All patches were secured using Bioclusive dressing (Systagenix Wound Management, Quincy, MA). For each subsequent measurement the patch was removed and the active site was cleaned with gauze, measurements were obtained followed by reapplication of gel and patch. Single measurements were obtained for all post treatment measurements to minimize the exposure of the active site to air and gel on the measurement electrode. Data was analyzed using the following equation for calculation of Z_{pores} (impedance of pores),

$$Z_{\text{total}} = \frac{1}{\frac{1}{Z_{\text{box}}} + \frac{1}{Z_{\text{skin}}} + \frac{0.02}{Z_{\text{pores}}}}$$

Where Z_{skin} was obtained from the intact skin value under the same treatment condition at each time point, $Z_{\text{box}}=200\text{k}\Omega$ resistance box and Z_{total} is the raw value obtained on the meter. Admittance (1/Impedance) values were used to compare pore closure kinetics among formulations. All data were reported as mean \pm SD.

2.9 Statistical analysis

Data for all experiments are reported as mean \pm standard deviation. Statistical analysis of data was carried out with Students' t-test and one way ANOVA with Tukey's posthoc pairwise tests, if required, using GraphPad Prism® software. $P<0.05$ was considered to be statistically significant.

Results

3.1 pH and viscosity measurements

The pH of all *in vitro* donor formulations was measured before and after addition of drug. Changes in formulation pH were observed for all solutions following the addition of the drug. The change was more significant for formulations at the lower end of the pH spectrum. The viscosity was also measured for all formulations to account for the effect of viscosity on MN enhanced transdermal flux. The lower pH formulations were more viscous, which can be attributed to the higher concentration of drug in those formulations. Viscosity decreased significantly with increase in formulation pH ($p<0.05$), except at pH 6.72 and pH 7.56($p>0.05$). Table 1 lists the changes in pH and viscosity for all formulations. The pH of each solution at dosing was used for all subsequent results and calculations.

3.2 Solubility measurements

The solubility of NTX was quantified in all *in vitro* donor solutions. Figure 1 shows the measured experimental values of solubility at 32°C for the 6 different pH conditions compared to the predicted values from Scifinder® at 25°C. The measured values were higher compared to the predicted values across the pH range.

3.3 *In vitro* diffusion studies

Flux was determined across MN treated skin as well as non-treated control for each of the 6 formulations (Figure 2). The flux values indicated that there was a significant difference in flux across MN treated skin among the formulations ($p < 0.05$), except for pH 5.76 compared to pH 6.3, and pH 7.56 compared to pH 8.26. Flux values across non-treated control skin were not significantly different from each other among the formulations ($p > 0.05$). Significant flux enhancement was obtained due to MN treatment at pH 5.76, pH 6.30, pH 6.43 and pH 6.72 as compared to intact skin control ($p < 0.05$).

Skin concentration and lag time were calculated from the *in vitro* studies. Table 2 lists the flux enhancement, skin concentration, and lag time of NTX across MN treated and non-treated skin. Flux enhancement was higher in lower pH/higher solubility formulations compared to the higher pH/lower solubility formulations. Skin concentration data for MN treated skin mimicked the flux profiles; formulations exhibiting higher flux had higher concentration of the drug in the skin. Skin concentrations for MN treated samples were significantly different from each other for all formulations ($p < 0.05$) except between pH 5.76 and pH 6.3, and pH 7.56 compared to pH 8.26. Skin concentrations for non-treated skin were not significantly different from each other ($p > 0.05$). The lag time calculations showed that MN treatment significantly reduced the lag time compared to non-treated control for all formulations except pH 7.56. Lag time also increased with increase in pH for MN treated skin ($p < 0.05$).

3.4 *In vivo* studies for pore closure kinetics

In vivo studies were conducted in a Yucatan miniature pig model to look at the effect of formulation pH on closure of micropores. Three different pH values were evaluated for impedance studies. The average raw values for pre and post MN treatment were 84.59 ± 17.82 and 25.87 ± 0.88 , respectively. Significant differences between pre and post MN treatment impedance values were obtained for all sites (data not shown) ($p < 0.05$). Figure 3 shows a plot of admittance values vs. time. The admittance values were significantly different between pH 5.5 and pH 6.5, and pH 5.5 compared to pH 7.4 at 24h ($p < 0.05$). There was no significant difference in admittance values between pH 5.5 and pH 7.4 beyond the 24h time point ($p > 0.05$).

Discussion

The current study was designed to look at the effect of formulation pH on transport and pore closure across MN treated skin. Formulation plays a significant role in any drug delivery system by having an effect on stability and solubility from the physicochemical standpoint, to ease of use from a clinical standpoint. Since this study focuses on effect of pH, the choice of the buffer was important and it was based on previous publications that studied the effect of pH on wound healing²³. The 3 pKa values associated with citrate buffer are 3.13, 4.76 and 6.4 and it is widely used in the pH range of 3–7. A single buffer species was chosen for all pH values to reduce variability in the data due to formation of a second NTX species following overnight incubation in saturated buffer solutions. *In vivo* studies were conducted at a buffer concentration of 0.1M, comparable to previous literature. Higher buffer strength of 0.3M was used for *in vitro* studies since the buffer strength of 0.1M was not suitable in

the presence of high concentrations of NTX base in solution. Changes in the final pH of the formulations following incubation with drug were noted and used for all subsequent calculations. Solubility of NTX base in the donor formulation was higher, compared to predicted values from Scifinder[®]. The difference in solubility can be explained in terms of the temperature difference. The predicted values were at 25°C, while the experimental values were at 32°C. The solubility could also be higher due to formation of NTX citrate following overnight incubation. The data reported in this paper is in agreement with previously published literature on solubility of NTX salts at 32°C¹⁶. Previous researchers also reported that saturation solubility is reached around pH 5.0; therefore the range of data in the current study is sufficient to explore the effect of formulation pH on flux and permeability for NTX.

The *in vitro* results showed that MN enhancement translated into significant flux enhancement at pH 5.76, pH 6.3, pH 6.43 and pH 6.72. The flux across MN treated skin was not significantly different from non-treated control for pH 7.56 and pH 8.26. Thus it can be concluded that formulation pH had an effect on flux enhancement across MN treated skin. The enhancement ratio of 11.24±2.9 at pH 5.76 indicated that using a lower pH formulation is advantageous in terms of flux enhancement across MN treated skin. Since flux enhancement directly translates into higher plasma concentration, this will lead to smaller patch sizes or fewer numbers of MN treatments in an individual.

MN enhanced drug delivery employs two distinctly different routes for drug transport, the microchannel pathway through the micropores created across the skin/SC barrier and passive transport through the intact skin pathway around the microchannels. However, since the SC is the most important barrier for transport for a large number of molecules, removing the SC barrier theoretically enhances permeability by 100–1000 times¹. The only exceptions to this rule are highly lipophilic molecules that form a depot in the SC and release slowly over time. Thus, the total flux (J_{TOT}) can be considered to be a sum of the flux values across two parallel routes, relative contribution of the MN pathway (J_{MCP}) and intact skin pathway (J_{ISP}) flux values towards the total flux can be obtained using the following equation¹⁴.

$$J_{TOT} = J_{MCP} + J_{ISP}$$

J_{ISP} is obtained from the intact skin (non-treated) control cells for each pH value. Subtracting the J_{ISP} from the total flux of MN treated cells at each pH value gives J_{MCP} . Fig 4 shows the relative contribution of the two different pathways towards the total flux across the pH range. At formulation pH 5.76 NTX is 98% ionized (pKa 7.5), while at pH 7.56 NTX is 50% ionized. Fig 4. shows that J_{MCP} is 91% of total flux at pH 5.76 and decreases to 13% at pH 7.56. As the percentage of ionized molecules decreased in formulation, the contribution of the J_{MCP} towards the total flux decreased. This can be explained in terms of the movement of ionized and unionized molecules across the skin. The MN treated skin drug permeates directly into the interstitial fluid in the microchannel pathway, a hydrophilic environment that facilitates permeation of hydrophilic molecules. Since solubility of the ionized form of the drug is significantly higher in an aqueous formulation, it translates into faster flux across MN treated skin at a lower pH. On the other hand, unionized molecules move faster through intact SC since charge on the surface of the molecule hinders its movement and partitioning¹. Skin concentration data exhibited a similar profile to flux for MN treated and non-treated skin. Thus, the higher flux at lower pH values is not an effect of saturation of the skin with NTX. Lag time measurements were obtained from the steady state profiles to compare formulations. The average lag time for non-treated skin was around 20h, while the lag time for the pH 5.76 condition in MN treated skin was 5h. Significantly

shorter lag times of low pH formulations in MN treated skin would be beneficial for development of a drug delivery system, since shorter lag times translate into shorter time to steady state plasma concentrations.

Permeability of drug across the skin barrier via the two different pathways would provide a better understanding of transport by eliminating the effect of solubility. Therefore, total permeability (P_{TOT}), microchannel pathway permeability (P_{MCP}), and intact skin pathway permeability (P_{ISP}) were calculated using the following equations.

$$J_{TOT} = P_{TOT} * S_{TOT} \quad J_{MCP} = (f_{MCP} * P_{MCP} * S_{TOT}) \quad J_{ISP} = (f_{ISP} * P_{ISP} * S_{TOT})$$

J_{TOT} , J_{MCP} and J_{ISP} were previously calculated values from Figure 4. The values of f_{MCP} and f_{ISP} were the fractional area of the treated skin exposed to active MN delivery and passive delivery, respectively. f_{MCP} has been estimated to be 0.02 or 2% of the total area and $f_{ISP} \sim 1$, based on prior literature³⁶. The total permeability of NTX across Yucatan pig skin as well as permeability via the two different routes was calculated. Figure 5 shows permeability values of NTX from each of the 6 different formulations. P_{MCP} was not calculated for pH 8.26 since the J_{MCP} calculation model does not allow for MN pathway flux calculation for that particular data point. The data showed that P_{MCP} was not significantly different among the formulations across the pH range ($p > 0.05$). On the other hand, P_{ISP} values for the higher pH formulation at pH 7.56 and pH 8.26 were significantly higher ($p < 0.05$), compared to the rest of the formulations. Thus P_{ISP} is affected by the change in ionization state of the molecule in formulation, and permeability of the unionized form of NTX is higher across intact skin compared to the ionized form. P_{MCP} is not influenced by the change in ionization state of the molecule indicating that transport across the MN pathway is independent of the ionization state. The flux enhancement observed at the lower pH formulations is solely a function of the higher solubility of the ionized form of the drug. At the higher pH values the flux/permeability is solely a function of the unionized species of the drug. This is evident from the fact that at pH 7.56 and pH 8.26 there is no significant difference between the P_{TOT} and P_{ISP} . The effect of charged and uncharged species on flux had already been studied before for MN treated skin. However, the current study looks at the role of speciation across the pH range to evaluate the effects in MN treated and non-treated skin, while controlling for important factors like viscosity of formulation, thickness of skin, etc.

Modeling the data in terms of permeability of the ionized and the unionized form of NTX would help in the mechanistic understanding of drug transport across MN treated and non-treated skin.⁴² The following model is used for calculating P_{MCP} and P_{ISP} . The total solubility of any molecule in solution is a function of the intrinsic solubility (S_{un}) and the solubility of the ionized form (S_i) of the molecule which is pH dependent. This assumes that only one pKa of NTX (pKa 7.5, associated with the protonation of the tertiary amine) is relevant for solubility calculations in the range of the experimental data. S_{un} (0.48mg/ml) was obtained from Scifinder[®] and S_i was calculated using the pKa and the pH values.

$$S_{TOT} = S_i + S_{un} \quad S_{TOT} = S_{un} \left(1 + \frac{H^+}{K_a} \right)$$

The S_{un} and S_i can then be used to calculate P_{MCP} and P_{ISP} utilizing the following equations. Model 1

$$J_{MCP} = (f_{MCP} * P_{MCP} * S_{TOT}) \quad J_{MCP} = \{f_{MCP} * (P_{MCPi} * S_i)\} + \{f_{MCP} * (P_{MCPun} * S_{un})\} \quad J_{ISP} = (P_{ISP} * S_{TOT}) \quad J_{ISP} = (P_{ISPi} * S_i) + (P_{ISPun} * S_{un})$$

Model 2

$$J_{MCP} = (f_{MCP} * P_{MCP} * S_{TOT}) \quad J_{MCP} = \{f_{MCP} * (P_{MCPi} * S_i)\} \quad J_{ISP} = (P_{ISP} * S_{TOT}) \quad J_{ISP} = (P_{ISPun} * S_{un})$$

The permeability of the ionized (P_{MCPi}) and unionized (P_{MCPun}) form of NTX across the microchannel pathway, and ionized (P_{ISPi}) and unionized (P_{ISPun}) form across the intact skin pathway were estimated using the experimental data. The permeability at pH 5.76 was used for the completely ionized form of the drug, and pH 8.26 was used for the completely unionized form of the drug. Since the P_{MCP} could not be calculated for pH 8.26, P_{ISP} at pH 8.26 was used for the P_{MCPun} and P_{ISPun} values. The model assumes that the products of ionized permeability and unionized solubility and vice versa are negligible for both equations. Flux values calculated using the above equations were divided by the total calculated solubility to get calculated permeability values. Model fitting was done using Scientist® version 3.0 and least squares fitting to experimental data. From the fitted data, goodness of fit was $r^2 > 0.8$ for estimation of microchannel pathway permeability and $r^2 > 0.9$ for estimation of intact skin pathway permeability. The results indicated that the model can be used to predict permeability of a molecule both across MN treated and non-treated skin. In figure 6 the black dashed line is the calculated permeability from model 1. The grey line is the calculated permeability considering only the ionized species for microchannel pathway and unionized species for intact skin pathway (model 2). From the model, the permeability across MN treated skin is best predicted using the completely ionized form of the drug. Total permeability across the MN pathway is better predicted by model 1 indicating that it is a function of both the ionized and the unionized form of the drug. For model 2, the predicted permeability at pH 7.26 due to the ionized component alone is much lower compared to the experimental values indicating that at the higher pH values unionized molecules have a significant contribution towards the MN pathway flux. The intact skin permeability value can be predicted by estimating permeability for the ionized and unionized form of the drug, or only the unionized form of the drug. There is no significant difference in the predicted values with/without taking the ionized species into consideration i.e. between model 1 and model 2. P_{ISPi} values at the lower end of the pH range estimated to be negative by model 1 were forced to zero in Figure 6. From Table 1 it can also be seen that permeability of the completely ionized species (P_{ISPi}) for the intact skin pathway is estimated to be negative, indicating that negligible permeation of the ionized species takes place via the intact skin pathway for this particular molecule. Thus model prediction of flux based on pH of formulation can be used for a whole range of molecules by estimating the permeability of the ionized and unionized species for the particular molecule experimentally. For the intact skin pathway, different equations can be used to predict permeability of the unionized species, such as the Potts and Guy equation, etc^{43, 44}. Once permeability is known flux can be calculated using total solubility values since the model shows that there is no significant difference between model 1 and model 2 for intact skin. For MN treated skin, a single experiment will be required to determine the permeability of the completely ionized component across the membrane of choice. Using a combination of the P_{MCPi} and the intact skin permeability, flux can then be predicted across the pH range using the above model. Thus the data can be used to minimize wet lab experiments and facilitate selection of candidates for MN enhanced and passive transdermal delivery based on their solubility and estimated permeability across the pH range.

Barrier recovery is one of the most important aspects of enhanced transdermal delivery systems like MN. The rate of healing of the skin determines the rate of delivery across the skin. Previously published reports have investigated the role of various factors in skin wound healing in different wound models ranging from acetone treatment to tape stripping and full thickness wounds. The role of pH was investigated in an acetone treated model of acute barrier perturbations and it was reported that barrier recovery was slower at pH 7.4 over a 6h period. The slower rate of recovery was attributed to lower activity of β -glucocerebrosidase and post secretory processing of lipids into lamellar membrane structures²³. However, this is only true when the SC barrier is completely destroyed and the skin loses its acidic environment. As the skin starts to recover and the acid mantle is reinstated the effects of external formulation pH are no longer observed. MN barrier disruptions are not well understood in terms of the pH environment of the wounds or barrier recovery. Thus the *in vivo* experiments in this paper were important to determine whether an external pH would have an effect on the rate of healing by affecting enzyme activity or post secretory processing over a prolonged period of time (7 days), thus extending the micropore lifetime. Impedance spectroscopy is a fairly new technique developed to look at wound healing or pore closure for MN channels, compared to TEWL. It has been used extensively to look at pore closure in rat models and humans¹⁹. Method development studies for impedance spectroscopy were also conducted to look at use of different electrodes, pressure of application, etc. in hairless guinea pigs, Yucatan miniature pigs, and humans⁴⁰. The current results showed that there was a significant difference between pH 5.5 and pH 7.4 at the 24 hour time point, but there were no significant differences in admittance values at 54h and 72h. Thus using a pH 7.4 formulation would not be beneficial for multiday pore lifetime enhancement in the current MN treatment model. The presence of certain cations, like calcium and potassium, has also been shown to have an effect on the rate of recovery indicating that ionic strength may also have an effect⁴⁵. In the current study citrate buffer was used and the pH of the buffer was adjusted with NaOH to eliminate effects of the different ions on barrier recovery. Interestingly the counter ion did not play a role in barrier recovery following iontophoresis⁴⁶.

Conclusion

The aim of the current study was to investigate the role of formulation pH on transport and recovery of MN treated skin. The *in vitro* results indicated that there is a significant flux advantage of using a lower pH, higher solubility (for a weak base) formulation for the development of a 7-day patch system. Modeling the data based on permeability gives an in depth understanding of the relative movement of the ionized and unionized form of the drug across MN treated and non-treated skin. The model can be further used for other drugs by obtaining permeability coefficients for the ionized and the unionized forms. The *in vivo* impedance spectroscopy data showed that there was no significant effect on barrier recovery/pore closure kinetics when using a higher pH formulation over the span of 4 days.

Acknowledgments

The authors would like to acknowledge Dr. Mark Prausnitz and Dr. Vladimir Zarnitsyn at the Georgia Institute of Technology for their expert advice and assistance with the MN arrays. Dr. Mikolaj Milewski provided advice on *in vitro* studies and Sophie (Xiujuan Peng), graduate student in Dr. Stephen Hoag's lab at University of Maryland, helped with viscosity measurements. This work was funded by NIH grants R01DA13425, R42DA32191, and University of Maryland, School of Pharmacy startup funding.

Literature Cited

1. Flynn, G. Anonymous Modern Pharmaceutics. Fourth Edition. Informa Healthcare; 2002. Cutaneous and Transdermal Delivery - Processes and Systems of Delivery.

2. Prausnitz MR, Langer R. Transdermal drug delivery. *Nat Biotech.* 2008; 26:1261–1268.
3. Elias PM, Cooper ER, Korc A, Brown BE. Percutaneous Transport in Relation to Stratum Corneum Structure and Lipid Composition. *J Investig Dermatol.* 1981; 76:297–301. [PubMed: 7205031]
4. Barry BW. Novel mechanisms and devices to enable successful transdermal drug delivery. *European Journal of Pharmaceutical Sciences.* 2001; 14:101–114. [PubMed: 11500256]
5. FAU BJ, Meinardi MM. The 500 Dalton rule for the skin penetration of chemical compounds and drugs. *Experimental dermatology JID--9301549.* 0925
6. Prausnitz MR, Mitragotri S, Langer R. Current status and future potential of transdermal drug delivery. *Nat Rev Drug Discov.* 2004; 3:115–124. [PubMed: 15040576]
7. Chen L, Han L, Lian G. Recent advances in predicting skin permeability of hydrophilic solutes. *Adv Drug Deliv Rev.*
8. Prausnitz MR. Microneedles for transdermal drug delivery. *Advanced Drug Delivery Reviews.* 2004; 56:581–587. [PubMed: 15019747]
9. Gomaa YA, Morrow DIJ, Garland MJ, Donnelly RF, El-Khordagui LK, Meidan VM. Effects of microneedle length, density, insertion time and multiple applications on human skin barrier function: Assessments by transepidermal water loss. *Toxicology in Vitro.* 2010; 24:1971–1978. [PubMed: 20732409]
10. Gill HS, Denson DD, Burris BA, Prausnitz MR. Effect of Microneedle Design on Pain in Human Volunteers. *The Clinical Journal of Pain.* 2008; 24:585–594. [PubMed: 18716497]
11. Banks S, Pinninti R, Gill H, Crooks P, Prausnitz M, Stinchcomb A. Flux Across Microneedle-treated Skin is Increased by Increasing Charge of Naltrexone and Naltrexol In Vitro. *Pharmaceutical Research.* 2008; 25:1964–1964.
12. Gupta JFAU, Felner, Eric I, FAU FE, Prausnitz MR. Minimally invasive insulin delivery in subjects with type 1 diabetes using hollow microneedles. *Diabetes technology & therapeutics JID--100889084.* 0917
13. Gill HS, Prausnitz MR. Coated microneedles for transdermal delivery. *J Controlled Release.* 2007; 117:227–237.
14. Milewski M, Stinchcomb A. Vehicle Composition Influence on the Microneedle-Enhanced Transdermal Flux of Naltrexone Hydrochloride. *Pharmaceutical Research.* 2011; 28:124–134. [PubMed: 20577787]
15. Li G, Badkar A, Nema S, Kolli CS, Banga AK. In vitro transdermal delivery of therapeutic antibodies using maltose microneedles. *Int J Pharm.* 2009; 368:109–115. [PubMed: 18996461]
16. Milewski M, Pinninti RR, Stinchcomb AL. Naltrexone salt selection for enhanced transdermal permeation through microneedle-treated skin. *J Pharm Sci.* 2012; 101:2777–2786. [PubMed: 22628183]
17. Banks SL, Pinninti RR, Gill HS, Paudel KS, Crooks PA, Brogden NK, Prausnitz MR, Stinchcomb AL. Transdermal delivery of naltrexol and skin permeability lifetime after microneedle treatment in hairless guinea pigs. *J Pharm Sci.* 2010; 99:3072–3080. [PubMed: 20166200]
18. Kalluri H, Banga A. Formation and Closure of Microchannels in Skin Following Microporation. *Pharmaceutical Research.* 2011; 28:82–94. [PubMed: 20354766]
19. Gupta JFAU, Gill, Harvinder S, FAU GH, FAU AS, Prausnitz MR. Kinetics of skin resealing after insertion of microneedles in human subjects. *Journal of controlled release : official journal of the Controlled Release Society JID--8607908.* 0606
20. Brogden NK, Milewski M, Ghosh P, Hardi L, Crofford LJ, Stinchcomb AL. Diclofenac Delays Micropore Closure Following Microneedle Treatment in Healthy Human Subjects. *Journal of Controlled Release.* 2012; 163(2):220–229. [PubMed: 22929967]
21. Feingold KR. The outer frontier: the importance of lipid metabolism in the skin. *J Lipid Res.* 2009; 50(Suppl):S417–S422. [PubMed: 18980941]
22. Broughton G II, Janis JE, Attinger CE. *The Basic Science of Wound Healing.* Plast Reconstr Surg. 2006; 117
23. Mauro T, Holleran WM, Grayson S, Gao WN, Man MQ, Kriehuber E, Behne M, Feingold KR, Elias PM. Barrier recovery is impeded at neutral pH, independent of ionic effects: implications for extracellular lipid processing. *Arch Dermatol Res.* 1998; 290:215–222. [PubMed: 9617442]

24. Holleran WM, Takagi Y, Imokawa G, Jackson S, Lee JM, Elias PM. beta-Glucocerebrosidase activity in murine epidermis: characterization and localization in relation to differentiation. *Journal of Lipid Research*. 1992; 33:1201–1209. [PubMed: 1431599]
25. Takagi Y, Kriehuber E, Imokawa G, Elias PM, Holleran WM. β -Glucocerebrosidase activity in mammalian stratum corneum. *Journal of Lipid Research*. 1999; 40:861–869. [PubMed: 10224155]
26. Grubauer G, Feingold KR, Harris RM, Elias PM. Lipid content and lipid type as determinants of the epidermal permeability barrier. *J Lipid Res*. 1989; 30:89–96. [PubMed: 2918253]
27. Elias PM, Tsai J, Menon GK, Holleran WM, Feingold KR. The Potential of Metabolic Interventions to Enhance Transdermal Drug Delivery. *J Investig Dermatol Symp Proc*. 2002; 7:79–85.
28. Schneider LA, Korber A, Grabbe S, Dissemond J. Influence of pH on wound-healing: a new perspective for wound-therapy? *Arch Dermatol Res*. 2007; 298:413–420. [PubMed: 17091276]
29. Gethin, G. The significance of surface pH in chronic wounds. Vol. 3. *Wounds UK*: 2007. p. 52
30. scifinder.cas.org: American chemical society
31. National Institute on Alcohol Abuse and Alcoholism. <http://www.niaaa.nih.gov>
32. PDR. second ed. New Jersey: Medical economics; 1996.
33. Alkermes Vivitrol (naltrexone for extended release injectable suspension). <http://www.vivitrol.com/>
34. Wermeling DP, Banks SL, Hudson DA, Gill HS, Gupta J, Prausnitz MR, Stinchcomb AL. Microneedles permit transdermal delivery of a skin-impermeant medication to humans. *Proceedings of the National Academy of Sciences*. 2008; 105:2058–2063.
35. Milewski M, Yerramreddy TR, Ghosh P, Crooks PA, Stinchcomb AL. In Vitro Permeation of a Pegylated Naltrexone Prodrug Across Microneedle-Treated Skin. *J Control Release*. 2010; 146:37–44. [PubMed: 20678989]
36. Milewski M. MICRONEEDLE-ASSISTED TRANSDERMAL DELIVERY OF NALTREXONE SPECIES: *IN VITRO* PERMEATION AND *IN VIVO* PHARMACOKINETIC STUDIES. 2012
37. Banks S, Paudel K, Brogden N, Loftin C, Stinchcomb A. Diclofenac Enables Prolonged Delivery of Naltrexone Through Microneedle-Treated Skin. *Pharmaceutical Research*. 2011:1–9.
38. Brogden NK. CLINICAL EVALUTION OF NOVEL METHODS FOR EXTENDING MICRONEEDLE PORE LIFETIME. 2012
39. Ghosh P, Pinninti RR, Hammell DC, Paudel KS, Stinchcomb AL. Development of a codrug approach for sustained delivery across microneedle treated skin. *J Pharm Sci*. 2013 Jan. Accepted.
40. Brogden NK, Ghosh P, Stinchcomb AL. Development of in vivo impedance spectroscopy techniques for measurement of micropore formation. *Journal of Investigative Dermatology*. 2012 Dec. Submitted.
41. Paudel KS, Nalluri BN, Hammell DC, Valiveti S, Kiptoo P, Hamad MO, Crooks PA, Stinchcomb AL. Transdermal delivery of naltrexone and its active metabolite 6- -naltrexol in human skin in vitro and guinea pigs in vivo. *Journal of Pharmaceutical Sciences*. 2005; 94:1965–1975. [PubMed: 16052561]
42. Hadgraft J, Valenta C. pH, pKa and dermal delivery. *Int J Pharm*. 2000; 200:243–247. [PubMed: 10867254]
43. Potts RO, Guy RH. Predicting skin permeability. *Pharm Res*. 1992; 9:663–669. [PubMed: 1608900]
44. Milewski M, Stinchcomb AL. Estimation of Maximum Transdermal Flux of Nonionized Xenobiotics from Basic Physicochemical Determinants. *Mol Pharm*. 2012
45. Mao-Qiang M, Mauro T, Bench G, Warren R, Elias PM, Feingold KR. Calcium and potassium inhibit barrier recovery after disruption, independent of the type of insult in hairless mice. *Exp Dermatol*. 1997; 6:36–40. [PubMed: 9067705]
46. Curdy C, Kalia YN, Falson-Rieg F, Guy RH. Recovery of human skin impedance in vivo after iontophoresis: effect of metal ions. *AAPS PharmSci*. 2000; 2:E23. [PubMed: 11741239]

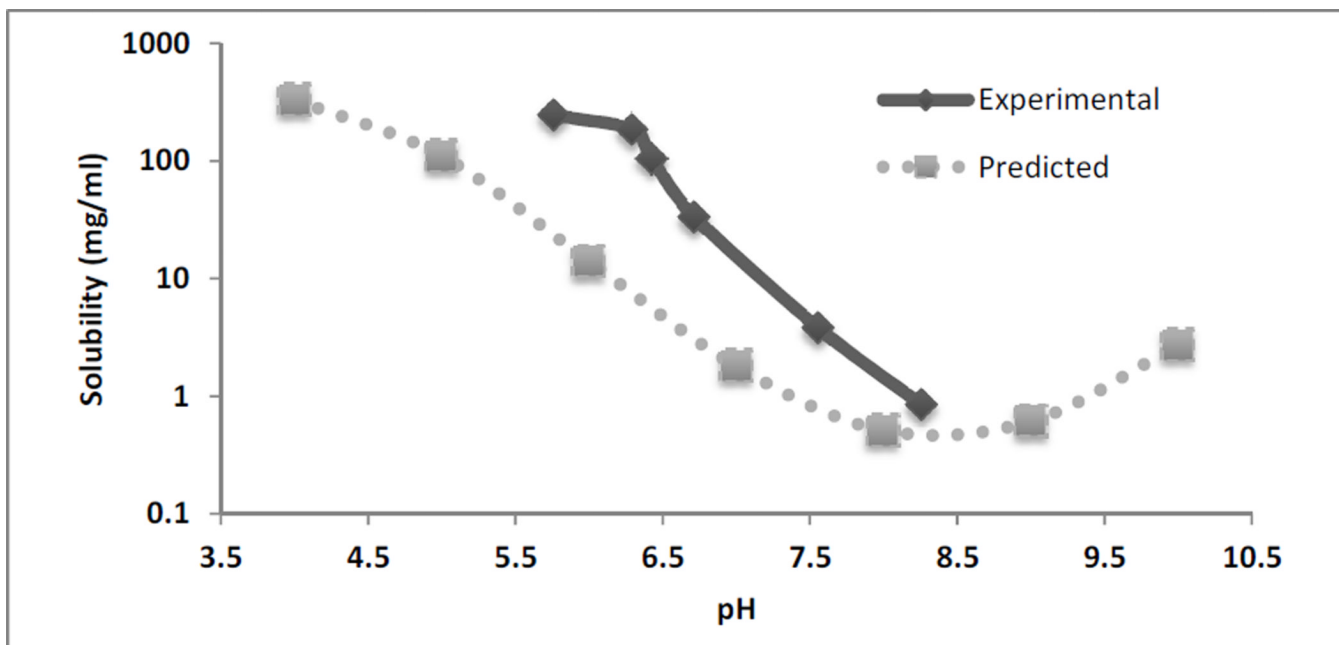


Fig 1. Solubility of NTX base in citrate buffer (0.3M) at 6 different values at 32°C. The dashed line represents the predicted values from Scifinder® in the pH range of 4–10 at 25°C. (n=3 for solubility determinations)

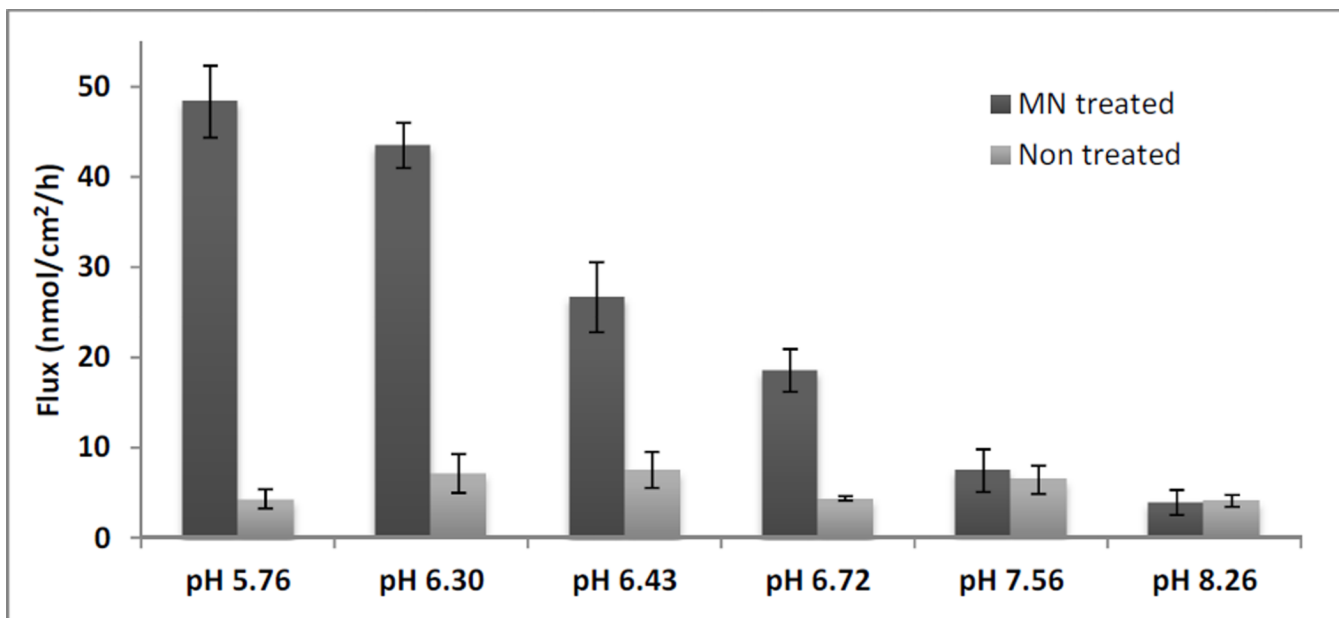


Fig 2. NTX flux across MN treated and non-treated pig skin from 6 different formulations (n=3–4). MN treated flux was significantly higher compared to non-treated skin for pH 5.76, pH 6.3, pH 6.43 and pH 6.72 ($p < 0.05$)

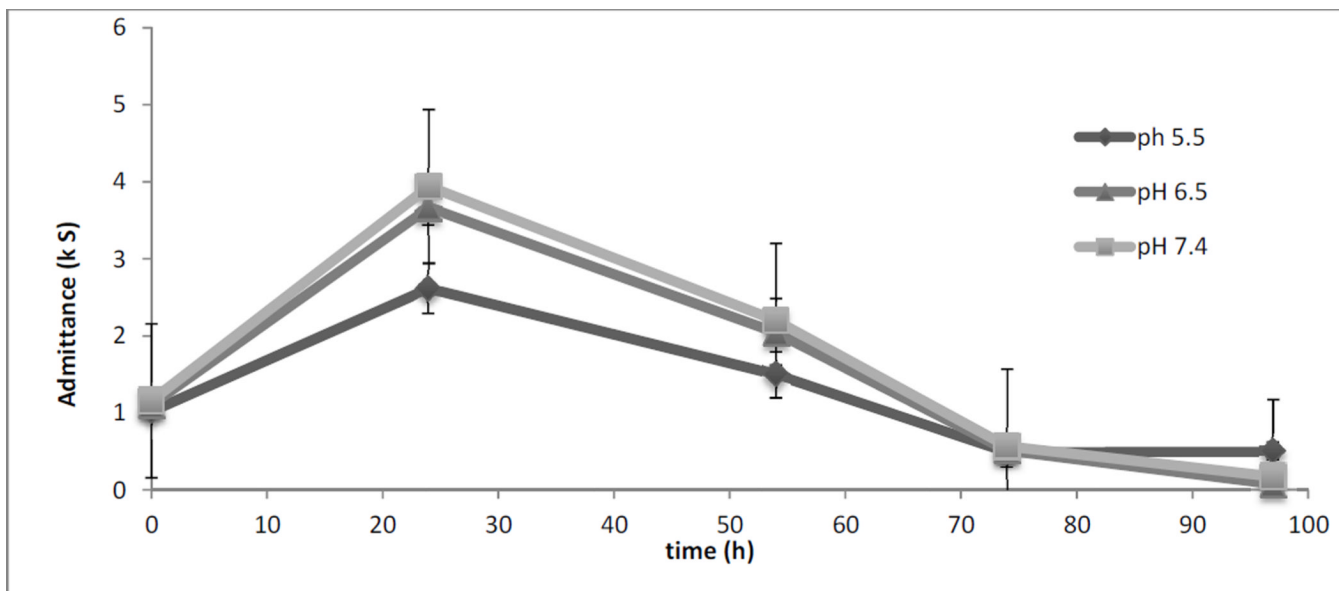


Figure 3. Admittance values vs. time for 3 different pH values. Admittance values were not significantly different from each other between the formulations ($p>0.05$) except for the 24h time point ($p<0.05$).

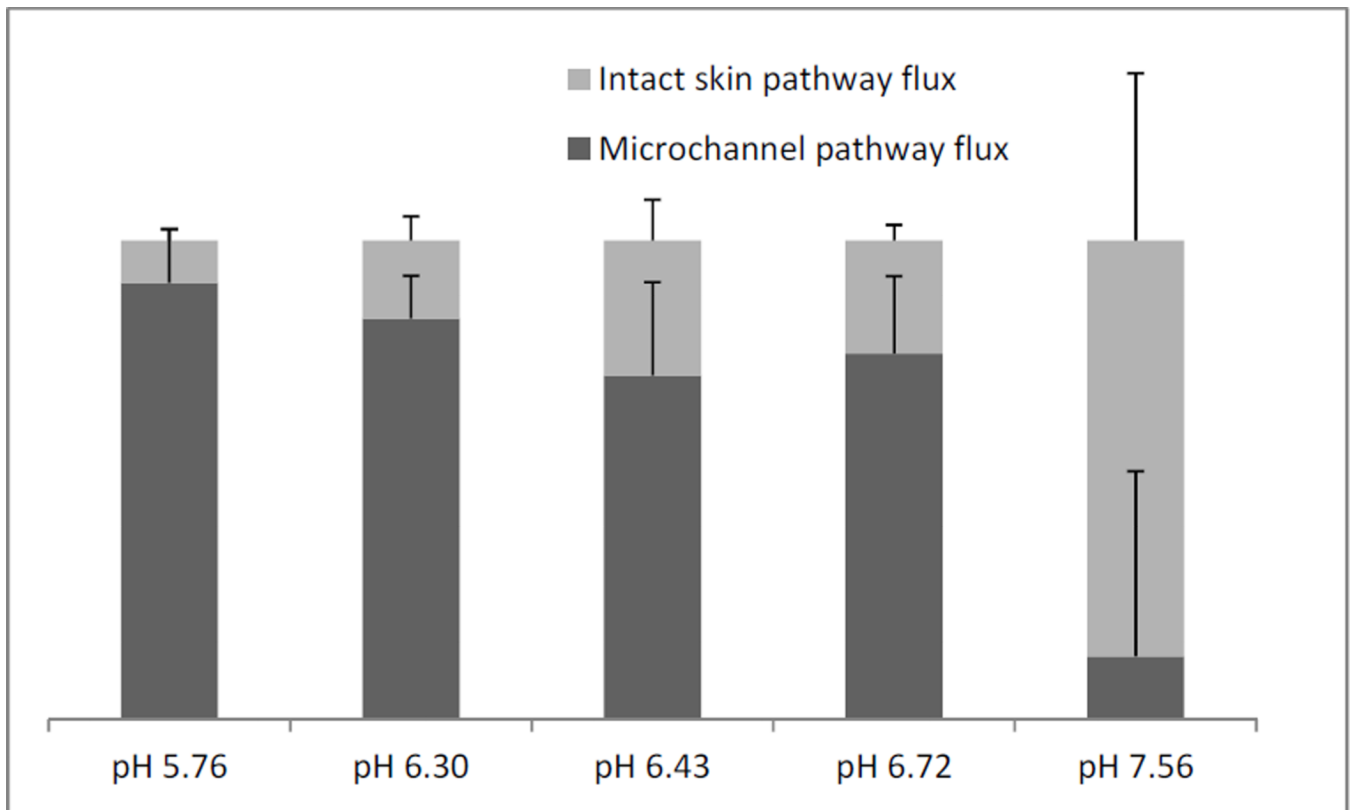


Figure 4. Relative contribution of microchannel pathway and intact skin pathway towards total flux from 5 different formulations.

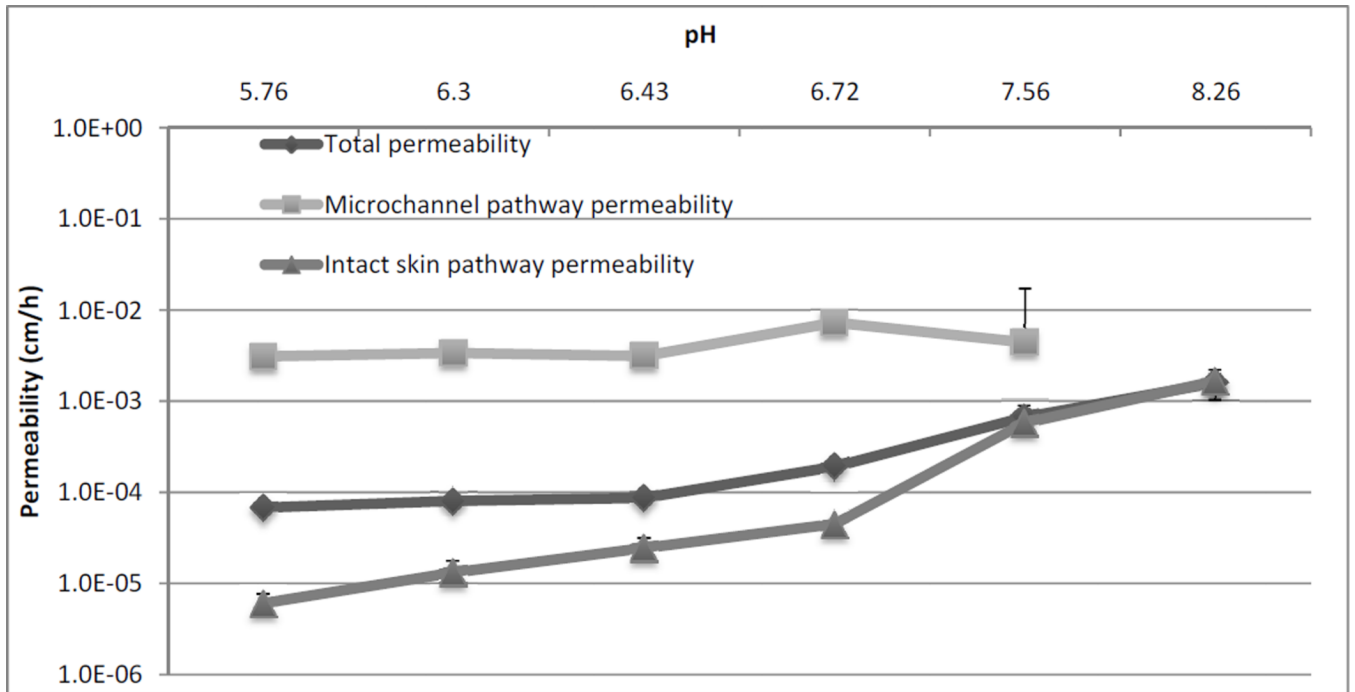


Figure 5.
Permeability of NTX across microchannel pathway and intact skin pathway

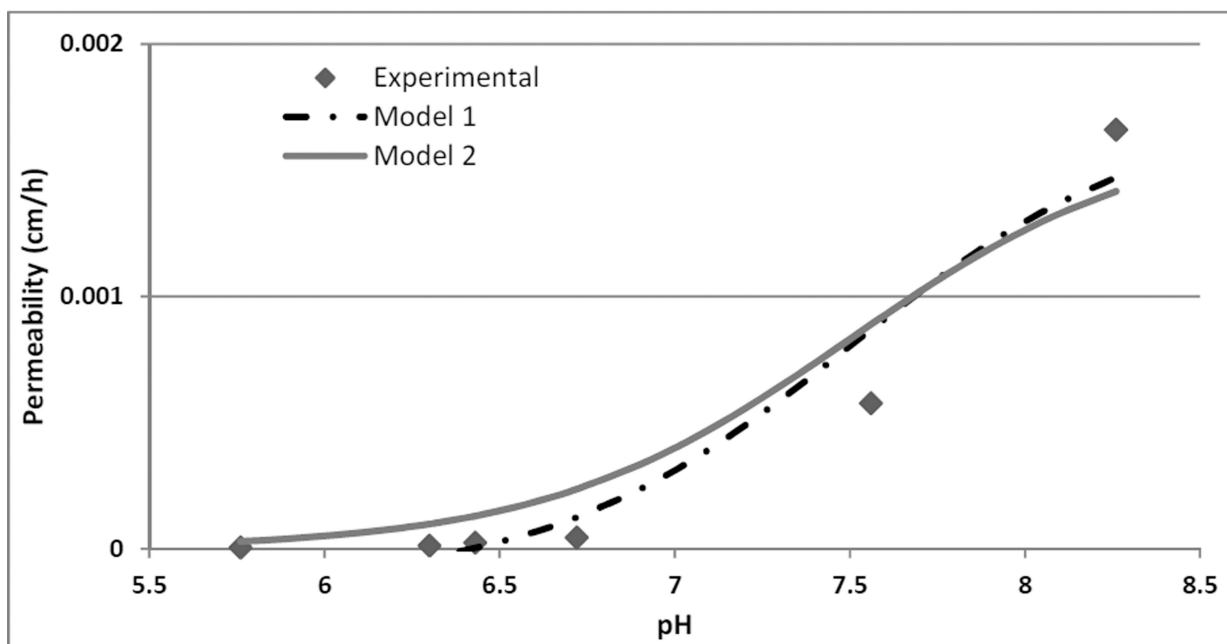
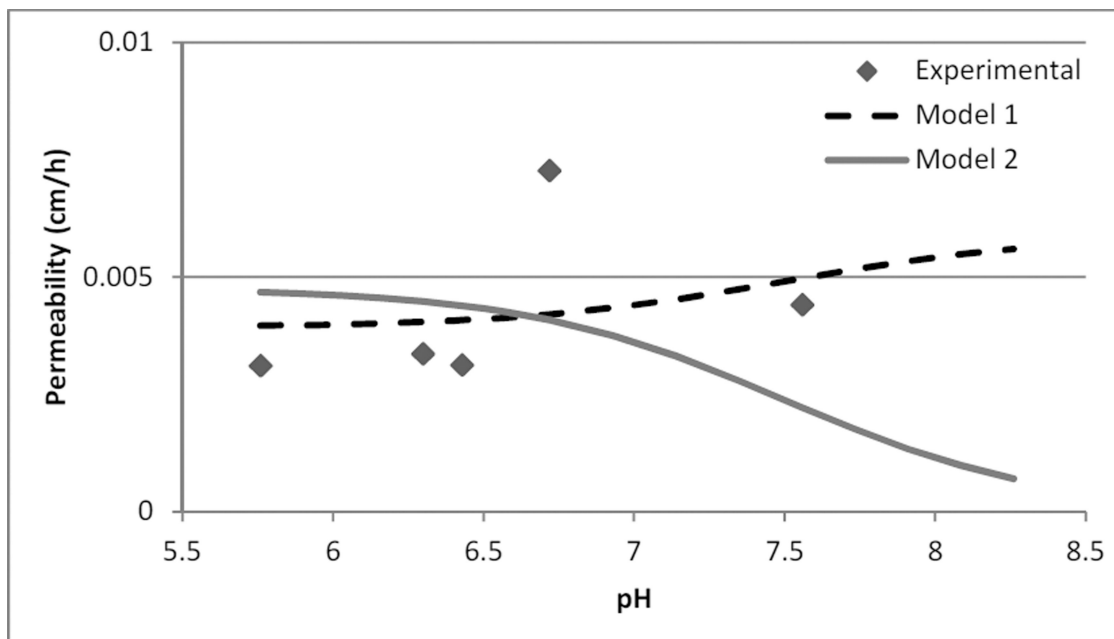


Figure 6. Permeability estimation of NTX species through the microchannel pathway (a) and intact skin pathway (b). The dashed black line is the calculated value of permeability based on model 1. The solid line is calculated permeability based on model 2. The points are the experimental parameters. Model selection criteria's for model 1 and model 2 respectively, MN treated skin -0.74 and -0.88 , intact skin 2.05 and 2.00 .

Table 1

Formulation characteristics of 6 different formulations (n=3 for all measurements).

pH of buffer	pH of formulation (after addition of drug)	Viscosity (cP)
2.3	5.76	4.01 ± 0.03
3.5	6.30	3.47 ± 0.02
4.5	6.43	2.57 ± 0.01
5.5	6.72	2.20 ± 0.02
6.5	7.56	2.22 ± 0.07
7.4	8.26	1.98 ± 0.0

Table 2

Diffusion parameters for 6 different formulations across MN treated and non-treated pig skin. (n=34).

pH of buffer	pH of formulation (after addition of drug)	Flux enhancement	Skin concentration ($\mu\text{mol/g}$)		Lag time (h)	
			MN treated	Non treated	MN treated	Non treated
2.3	5.76	11.24 \pm 2.90	5.15 \pm 0.48	2.11 \pm 1.14	5.01 \pm 2.76	21.26 \pm 0.16
3.5	6.30	6.11 \pm 1.87	5.22 \pm 0.46	2.12 \pm 0.15	6.41 \pm 0.80	16.27 \pm 0.68
4.5	6.43	3.55 \pm 1.07	3.99 \pm 0.54	2.98 \pm 1.31	6.09 \pm 3.12	18.24 \pm 3.76
5.5	6.72	4.24 \pm 0.59	2.96 \pm 0.38	1.09 \pm 0.18	10.89 \pm 0.67	21.64 \pm 1.34
6.5	7.56	1.15 \pm 0.46	1.44 \pm 0.29	1.43 \pm 0.12	19.24 \pm 2.21	22.59 \pm 0.26
7.4	8.26	0.96 \pm 0.37	0.79 \pm 0.22	0.96 \pm 0.15	20.85 \pm 2.32	24.76 \pm 1.12

Table 3

Experimental and calculated permeability values from model 1 and model 2

	Experimental	Model 1	Model 2
P_{MCPi} (cm/h)	$3.10 \times 10^{-3} \pm 3.25 \times 10^{-4}$	$3.92 \times 10^{-3} \pm 1.18 \times 10^{-3}$	$4.75 \times 10^{-3} \pm 1.18 \times 10^{-3}$
P_{MCPun} (cm/h)	$1.66 \times 10^{-3} \pm 2.70 \times 10^{-4}$	$5.89 \times 10^{-3} \pm 4.0 \times 10^{-3}$	-----
P_{ISPi} (cm/h)	$6.06 \times 10^{-6} \pm 1.51 \times 10^{-6}$	$-(1.45 \times 10^{-4}) \pm 1.05 \times 10^{-4}$	-----
P_{ISPun} (cm/h)	$1.66 \times 10^{-3} \pm 2.70 \times 10^{-4}$	$1.75 \times 10^{-3} \pm 1.96 \times 10^{-4}$	$1.66 \times 10^{-3} \pm 2.02 \times 10^{-4}$